CHARACTERIZING THE EFFECT OF BORTEZOMIB ON RIFT VALLEY FEVER VIRUS MULTIPLICATION

by

Forrest David Keck
A Thesis
Submitted to the
Graduate Faculty
of
George Mason University
in Partial Fulfillment of
The Requirements for the Degree
of
Master of Science
Biology

Committee:

_____	Dr. Aarthi Narayanan
	Thesis Director
_____	Dr. Anne Verhoeven
	Committee Member
_____	Dr. Ramin Hakami
	Committee Member
_____	Dr. James D. Willett
	Director, School of Systems Biology
_____	Dr. Donna M. Fox
	Associate Dean, Office of Student Affairs & Special Programs
_____	Dr. Peggy Agouris
	Dean, College of Science
Date: _____	Spring Semester 2015 George Mason University Fairfax, VA

Characterizing the Effect of Bortezomib on Rift Valley Fever Virus Multiplication

A Thesis submitted in partial fulfillment of the requirements for the degree of Master of Science at George Mason University

by

Forrest David Keck
Bachelor of Science
George Mason University, 2013

Director: Aarthi Narayanan, Professor
School of Systems Biology

Spring Semester 2015
George Mason University
Fairfax, VA

DEDICATION

This is dedicated to my mother, Sarah, my high school Biology teacher, Dr. Walck, and my best friend, Colleen.

ACKNOWLEDGEMENTS

I would like to thank the many supporters who have made this thesis happen. My principal investigator, Dr. Narayanan, who taught me how to think like a graduate student and address complex biological issues in a methodical manner. Moushimi Amaya, whose open ears, vast skills repertoire, and patience were invaluable to the completion of my work. Drs. Kehn-Hall and Verhoeven, for inspiring me to continue in the field of infectious diseases. Finally I would like to thank all of my friends in Mason's Infectious Disease program whose critique and suggestions encouraged growth in my science ventures.

TABLE OF CONTENTS

LIST OF FIGURES

LIST OF ABBREVIATIONS AND SYMBOLS

4',6-diamindino-2-phenylindole fluorescent nuclear stain ..... DAPI
Carbon dioxide ..... CO_2
CREB binding protein ..... CBP
Cyclic adenosine monophoshpate response element-binding protein ..... CREB
Degrees Celsius ..... ^oC
Delta delta C_T ..... $\Delta\Delta$ C_T
Delta ..... Δ
Deoxyribose nucleic acid ..... DNA
Dimethyl Sulfoxide ..... DMSO
Distilled water ..... diH_2O
Dulbecco's Modified Eagle Medium ..... DMEM
Essential Modified Eagle Medium ..... EMEM
Ethylenediaminetetraacetic acid ..... EDTA
Fetal Bovine Serum ..... FBS
Flag-tagged NSs rMP-12 ..... FLAG-NSs-rMP-12
Food and Drug Administration ..... FDA
Glyceraldehyde 3-phosphate dehydrogenase ..... GAPDH
Histone deacetylase 3 ..... HDAC3
Horseradish peroxidase ..... HRP
Hours post infection ..... hpi
Human small airway epithelial cells ..... HSAECs
Immunoglobulin G ..... IgG
Immunoprecipitates ..... IPs
Interferon beta ..... IFN-β
Kilodalton ..... kDa
Microliter ..... µL
Micromolar ..... µM
Milligrams ..... mg
Milliliter ..... mL
Mulitplicity of infection ..... MOI
Nonstructural S protein ..... NSs
Nonyl phenoxypolyethoxylethanol 40 detergent NP-40
Nuclear receptor co-repressor 1 ..... NCoR
Plaque forming unit ..... PFU
Qualitative real time polymerase chain reaction ..... qRT-PCR
Recombinant mouse passage 12 attenuated Rift Valley Fever Virus rMP-12

Revolutions per minute ..... rpm
Ribonucleic acid ..... RNA
Rift Valley Fever Virus ..... RVFV
Sin3 transcription regulator family member A mSin3A
Sin3A-associated protein, 30 kDa SAP30
Sodium chloride ..... NaCl
Sodium dodecyl sulfate polyacrylamide gel electrophoresis ..... SDS-PAGE
Sodium fluoride ..... NaF
Sodium orthovanadate ..... Na_3VO_4
Threshold value ..... C_T
Transcription factor IIH ..... TFIIH
Trisaminol hydrochloric acid ..... Tris-HCl
Tris-HCl, NaCL, EDTA containing buffer ..... TNE
Ubiquitin Proteasome System ..... UPS
Whole cell extract ..... WCE
Yin Yang 1 transcriptional repressor protein YY1

ABSTRACT

CHARACTERIZING THE EFFECT OF BORTEZOMIB ON RIFT VALLEY FEVER VIRUS MULTIPLICATION

Forrest David Keck, M.S.

George Mason University, 2015

Thesis Director: Dr. Aarthi Narayanan

This thesis investigates the FDA-approved cancer drug Bortezomib; characterizing its use as a novel application in Bunyavirus antiviral therapy. Rift Valley Fever virus (RVFV) belongs to the family *Bunyaviridae* and is a known cause of epizootics and epidemics in Africa and the Middle East. With no FDA approved therapeutics available to treat RVFV infection, understanding the interactions between the virus and the infected host is crucial to developing novel therapeutic strategies. Here, we investigated the requirement of the ubiquitin-proteasome system (UPS) for the establishment of a productive RVFV infection. It was previously shown that the UPS plays a central role in RVFV multiplication involving degradation of PKR and p62 subunit of TFIIH. Using the FDA-approved proteasomal inhibitor Bortezomib, we observed robust inhibition of intracellular and extracellular viral loads. Bortezomib treatment did not affect the nuclear/cytoplasmic distribution of the non-structural protein NSs; however, the ability of

NSs to form nuclear filaments was abolished as a result of Bortezomib treatment. *In silico* ubiquitination prediction analysis predicted that known NSs interactors (SAP30, YY1, and mSin3A) have multiple putative ubiquitination sites, while NSs itself was not predicted to be ubiquitinated. Immunoprecipitation studies indicated a decrease in interaction between SAP30 – NSs, and mSin3A – NSs in the context of Bortezomib treatment. This decrease in association between SAP30 - NSs also correlated with a decrease in the ubiquitination status of SAP30 with Bortezomib treatment. Bortezomib treatment, however; resulted in increased ubiquitination of mSin3A, suggesting that Bortezomib dynamically affects the ubiquitination status of host proteins that interact with NSs. Finally, we observed that expression of interferon beta (IFN-β) was increased in Bortezomib treated cells which indicated that the cellular antiviral mechanism was revived as a result of treatment and may contribute to control of viral multiplication.

CHAPTER ONE: INTRODUCTION

Rift Valley Fever Virus

Rift Valley Fever Virus (RVFV) is a bunyavirus and considered to be an emerging pathogen of health relevance worldwide (Ikegami and Makino, 2011). RVFV is a zoonotic, mosquito-borne virus which causes epizootics and associated human epidemics in sub-Saharan Africa and the Arabian Peninsula (Indran and Ikegami, 2012; Pepin et al., 2010). Transmitted primarily by the *Aedes* and *Culex* species of mosquito, if bitten, human hosts typically display mild flu-like symptoms (Pepin et al., 2010). Additional clinical signs can develop, including: hepatitis, retinitis, and delayed-onset encephalitis (Pepin et al., 2010). In the most severe cases of RVFV, hemorrhagic fever may develop, although case fatality rates in humans is only estimated to be 2% (Pepin et al., 2010). In livestock, RVFV infections result in high mortality in young animals, and high rates of abortion (Pepin et al., 2010). As the mosquito vectors necessary for transmitting RVFV are already present in the United States, RVFV is classified as an overlap priority agent by the Centers for Disease Control and Prevention and the US Department of Agriculture (Indran and Ikegami, 2012). There are no FDA approved therapeutics for the treatment of RVFV infections; however, MP-12, a live attenuated form of the virulent ZH548 strain of RVFV is provided as a vaccine to at risk personnel (Pepin et al., 2010).

RVFV is a negative-stranded RNA virus, with a tripartite, single-stranded genome divided into the S, M, and L segments (Bouloy and Weber, 2010). The ambisense S segment encodes the N protein (NP) and the NSs nonstructural protein (Vialat et al., 2000). The M segment encodes the Gn and Gc envelope glycoproteins, a 78kD minor structural protein, and the NSm nonstructural protein (Pepin et al., 2010). The L segment encodes the viral RNA-dependent RNA polymerase (Pepin et al., 2010).

RVFV NSs protein, although dispensable to viral replication, has been demonstrated to be a critical virulence factor that enables the establishment of a productive infection by multiple mechanisms (Bird et al., 2008; Vialat et al., 2000). NSs suppressed transcription of host mRNA via the transcription factor IIH (TFIIH) subunit p44 and degradation of subunit p62 (Billecocq et al., 2004; Kainulainen et al., 2014; Kalveram et al., 2011; Le May et al., 2004). NSs also down regulated IFN-β expression in infected cells. This has been demonstrated to involve host chromatin remodeling factors and the assembly of NSs as characteristic filaments on the interferon promoter (Billecocq et al., 2004; Mansuroglu et al., 2010). Additionally, NSs induced the degradation of the double-stranded RNA-dependent protein kinase (PKR) (Habjan et al., 2009; Ikegami et al., 2009a, 2009b).

NSs is unique among bunyaviral proteins in its ability to form filamentous structures in the nucleus, interacting specifically with clusters of pericentromeric γ-satellite sequence (Mansuroglu et al., 2010; Struthers and Swanepoel, 1982; Swanepoel and Blackburn, 1977). NSs filaments are formed on DNA not by direct interaction of NSs with DNA, but via protein:protein interactions between NSs and chromatin remodeling

components (Mansuroglu et al., 2010). Specifically on the interferon promoter, NSs blocked IFN-β gene expression via its interactions with the IFN-β co-repressor complex. This complex, comprised of SAP30, YY1, HDAC3, NCoR, and mSin3A, blocked the co-activator, CREB binding protein (CBP) from binding the IFN-β promoter and facilitating transcriptional repression (Le May et al., 2008). Transcription repression by NSs has also been shown to involve NSs interaction with the p44 subunit of TFIIH, sequestering it and repressing cellular transcriptional activity (Ikegami et al., 2009a).

Repurposing FDA Approved Drugs

There are no FDA-approved therapies to treat RVFV infection; however, recent research has indicated the importance of host factors to RVFV multiplication and provided proof of concept evidence of the efficacy of host-based inhibitors against RVFV infections (Baer et al., 2012; Narayanan et al., 2012; Nuss et al., 2014; Popova et al., 2010). Bortezomib is an FDA-approved inhibitor of the 26S subunit of the proteasome, which has shown antiviral activity against multiple viruses (Adams and Kauffman, 2004; Bandi et al., 2010; Dudek et al., 2010; Raaben et al., 2010; Teale et al., 2009; Wang et al., 2010). In the light of multiple lines of evidence that the host proteasomal machinery is likely to be of importance to RVFV multiplication (Habjan et al., 2009; Ikegami et al., 2009a; Kainulainen et al., 2014; Kalveram et al., 2011), we hypothesized that Bortezomib will be a potent inhibitor of RVFV multiplication and the mechanism of inhibition will likely involve loss of NSs function.

We have determined that Bortezomib inhibits extracellular and intracellular viral titers. We demonstrate that Bortezomib treatment interfered with the ability of NSs to

form nuclear filaments in infected cells although this outcome is not the result of compromised NSs nuclear/cytoplasmic distribution. As such, we hypothesized that ubiquitination of host proteins will be necessary for assembly of NSs nuclear filaments. *In silico* analysis indicated that the known NSs interactors, mSin3A, YY1, and SAP30 could be ubiquitinated. We determined that Bortezomib altered the interaction between NSs-SAP30, and NSs- mSin3A, but not NSs-YY1. We also noticed a decrease in the ubiquitination status of SAP30 with Bortezomib treatment while it increased with mSin3A. Additionally, with Bortezomib treatment, we noted a recovery of IFN-β, which probably sets up an antiviral phenotype in treated cells and hence inhibits viral multiplication.

CHAPTER TWO: MATERIALS AND METHODS

Viruses and Cell Lines

The MP-12 strain of RVFV, was obtained as the result of 12 serial passages of the virulent ZH548 strain in the presence of 5-fluorouracil (Caplen et al., 1985; Vialat et al., 1997). The other strain used in this study, Flag-NSs, has a C-terminal Flag-tagged NSs inserted in place of NSs in the MP-12 backbone (Ikegami et al., 2009b). Human small airway epithelial cells (HSAECs) were maintained in Ham's F-12, 10% Fetal Bovine Serum (FBS), 1% Penicillin/Streptomycin, 1% Sodium Pyruvate, 1% L-Glutamine, 1% Non-essential amino acids, and 0.1% β-Mercaptoethanol at 37^{o}C, 5% CO_2. Vero cells were maintained in DMEM containing 10% FBS, 1% Penicillin/Streptomycin, and 1% L-Glutamine at 37^{o}C, 5% CO_2.

Cell Viability Assay

Viability for HSAECs was determined using Promega's CellTiter Glo assay, as previously described (Narayanan et al., 2012). This assay quantitates ATP levels, which directly reflects the level of cellular metabolic activity ("CellTiter-Glo Luminescent Cell Viability Assay," 2012).

Plaque Assay

Infectious particles from culture supernatants were quantified by plaque assay. Vero cells were seeded in a 12-well plate format. The next day, dilutions of culture supernatants were made in DMEM, and applied to wells. Plates were incubated at 37^{o}C,

5% CO_2 for 1 hour with rocking every 20 minutes. A 1 ml overlay comprising of 2X E-MEM and 0.6% agarose (1:1) was added to each well. The plates were incubated for an additional 72 hours at 37^oC, 5% CO_2. Following incubation, cells were fixed by applying a 10% Formaldehyde solution for 1 hour at room temperature. The agarose plugs were removed by rinsing with diH_2O. A 1% crystal violet solution was added to each well for 30 minutes at room temperature. The plates were rinsed with diH_2O and visible plaques were counted to determine viral titers as PFU/mL.

Immunoprecipitation

HSAECs were infected with Flag-NSs-MP-12 virus (MOI: 5) and maintained at 37^oC, 5% CO_2 for 24 hours. Cells were pelleted and lysed in a buffer containing Tris-HCL (pH 7.5), NaCl (120mM), EDTA (5 mM), NP-40 (0.5%), NaF (50 mM), Na_3VO_4 (0.2 mM), and one tablet complete proteasome inhibitor cocktail per 50ml. Lysis was performed on ice for 20 minutes. Cells were centrifuged at 4^oC for 10 minutes at 10,000 rpm. Total protein was quantified via Bradford assay (BioRad). Whole cell extract (2 mg) was pre-cleared and incubated overnight, rotating, at 4^oC with α-IgG, or α-Flag antibody (Sigma Aldrich, Cat# F3165). 50µl of Protein A+G beads were added to the immunoprecipitates (IPs) and incubated for 2 hours, rotating, at 4^oC. The IPs were centrifuged at 4^oC at 7000 rpm, and beads were washed 1x with TNE150+0.1% NP-40, followed by 2x washes with TNE50+0.1% NP-40.

Nuclear Cytoplasmic Fractionation

HSAECs were lysed with 200µL of lysis buffer (50mM Tris-HCl pH 7.5, 0.5% Triton X-100, 137.5mM NaCl, 10% Glycerol, 1mM $NaVaO_4$, 50 mM NaF, 10 mM

sodium pyrophosphate, 5mM EDTA, and protease inhibitor cocktail tablet). Cells were gently pipetted until the solution was homogenous prior to a 15 minute incubation on ice. Insoluble nuclei were separated via centrifugation at 3,000rpm for 5 min at 4^{o}C. The supernatant (cytoplasmic fraction) was transferred to a new centrifuge tube. The nuclear pellet was washed once with lysis buffer prior to re-suspension and homogenization in 200μL of lysis buffer. The nuclear fraction was isolated by centrifugation for 15 min at 13,000rpm and 4^{o}C. Fractions were analyzed via Western Blot for proteins of interest.

Immunofluorescence

Immunofluorescence studies were performed as previously described (Amaya et al., 2014). HSAECs were probed with anti-Flag antibodies, prior to incubation with Alexa-Fluor 488. The cells were stained with DAPI to observe the nuclei. Images were taken using a Nikon Eclipse TE2000-U with a 60X objective.

Western Blot Analysis

Western blot analysis for whole cell or fractionated lysates was carried out as previously described (Narayanan et al., 2014). Immunoprecipitated lysates were separated on a 14% Tris-Glycine gel for optimal resolution of proteins of interest. Primary antibodies to Flag (Sigma Aldrich), YY1 (Abcam, Cat# ab12132), mSin3A (Abcam, Cat# ab3479), SAP30 (Abcam, Cat# ab16047), GAPDH (Cell Signaling, Cat# 5174S), Lamin A/C (Cell Signaling, Cat# 4777S), Ubiquitin (Abcam, Cat# ab7780), and HRP-conjugated β-actin (Abcam, Cat# ab49900), were used according to manufacturer's instructions.

Quantitative RT-PCR for Viral RNA

RNA extraction was performed with Ambion's MagMax 96-well Viral RNA extraction kit (Life Technologies) according to the manufacturer's instructions. To determine the number of viral genomic copies produced, M-segment specific primers were used in conjunction with RNA UltraSense One-Step Quantitative RT-PCR System (Life Technologies) and a standardized protocol as previously described (Shafagati et al., 2013).

Quantitative RT-PCR for Host RNA

Cells were lysed using Ambion's MagMax 96-well Total RNA extraction kit (Life Technologies) according to the manufacturer's instructions. To determine the quantity of IFN-β produced, qRT-PCR with host specific IFN-β primers was performed using Superscript III Platinum Sybr Green One Step qPCR Kit with ROX (Life Technologies). The experiment was performed according to a standardized protocol using 20 µl of master mix containing SuperScript III RT/Platinum Taq mix, 2X SYBR Green Reaction Mix with ROX, 10 µM forward IFN-β primer (AAACTCATGAGCAGTCTGCA), and 10 µM reverse IFN-β primer (AGGAGATCTTCAGTTTCGGAGG), added to 5 ng/µl of extracted RNA. The samples were heated at 50^{o}C for 3 minutes, 95^{o}C for 5 minutes; and at 95^{o}C for 15 seconds and 60^{o}C for 30 seconds for 40 cycles. IFN-β results were quantitated using the ΔΔCt method against the β-actin endogenous control.

Statistical Analysis

All individual experiments were performed in triplicate, unless otherwise noted. Data points were averaged and the mean was graphed. Error bars represent standard

deviations calculated from the three independent experiments. Comparisons between treatment groups were carried out using the unpaired, two-tailed Students *t*-test, where *P* values were calculated using GraphPad's QuickCalcs software. Statistical significance was set at $P<0.05$. All significant results are indicated with an asterisk (*).

CHAPTER THREE: RESULTS AND DISCUSSION

Bortezomib treatment decreases RVFV viral titers in HSAECs

Bortezomib is a FDA approved specific, reversible inhibitor of the human proteasome (Adams and Kauffman, 2004). In order to evaluate the therapeutic potential of Bortezomib for the treatment of RVFV infections, we first determined its toxicity in HSAECs, a cell line that has been demonstrated to be a useful model for the study of RVFV infections (Baer et al., 2012; Narayanan et al., 2012, 2011; Popova et al., 2010). HSAECs were treated with 0.01 or 0.1μM, concentrations of Bortezomib for 24 hours after which survival was measured using the CellTiter Glo assay. The results indicated that with 0.01μM Bortezomib concentration, 90% of the treated cells survived when compared to the DMSO control (Figure 1A). For all of the subsequent experiments, Bortezomib was used at a final concentration of 0.01 μM unless indicated otherwise. The efficacy of Bortezomib to inhibit rMP-12 (MOI 0.1) multiplication was evaluated. Bortezomib was added 2 hours prior to infection for all experiments unless otherwise noted. Bortezomib treatment resulted in a statistically significant 2 log decrease in extracellular viral titers (Figure 1B). The ability of Bortezomib to inhibit viral multiplication was independent of viral titers as high MOIs of infection (MOI:1 and MOI:5) also produced a robust inhibition of viral multiplication (Figure 1C).

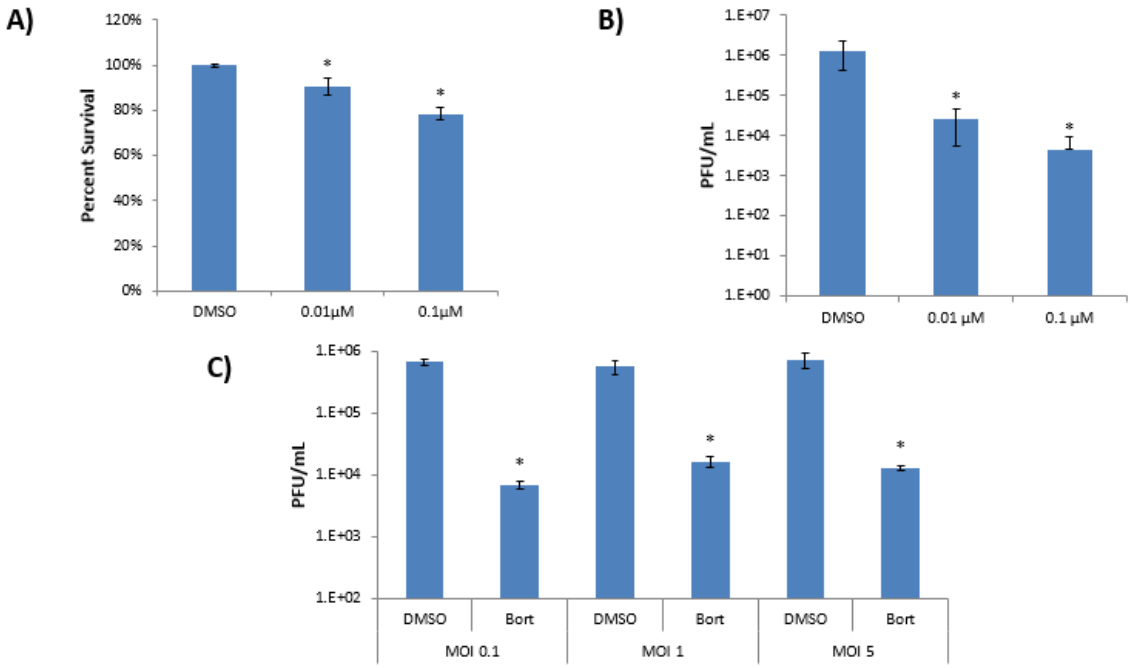

Figure 1: Toxicity and efficacy of Bortezomib in HSAECs. (A). HSAECs treated with 0.1% DMSO, 0.01µM or 0.1µM Bortezomib, in triplicate, and incubated for 24 hours. Cells were then analyzed for survival via CellTiter Glo assay. The graph represents the average of 3 independent experiments with each experiment conducted as biological triplicates. **(B).** HSAECs were either pre-treated with 0.1% DMSO, 0.01µM or 0.1µM Bortezomib for 2 hours. The conditioned media were removed prior to infection with rMP-12 (MOI 0.1) for 1 hour. Supernatants were collected at 24 hours and infectious viral titers (PFU/mL) determined. Results are an average of 2 independent experiments with biological triplicates. Standard deviations were calculated from 2 independent experiments. **(C).** HSAECs were pre-treated with 0.1% DMSO (control) or 0.01µM Bortezomib, for 2 hours. Cells were infected with rMP-12 (MOI 0.1, 1, or 5). Supernatants were collected 24hpi, and infectious viral titers determined. Standard deviations were calculated from 3 independent experiments. * indicates $P<0.05$.

As a next step, we quantified the viral replication kinetics of rMP-12 in the presence of Bortezomib. HSAECs were pre-treated with DMSO or Bortezomib, infected with rMP-12 (MOI: 0.1), supernatants collected at specified intervals post infection and infectious titers determined by plaque assays (Figure 2A). The results indicated a strong decrease in infectious viral titers at all time points analyzed with significant drops in viral titers recorded between 16 and 30 hours post infection (hpi). In order to determine if the

drop in extracellular infectious virus titers correlated with a decrease in intracellular viral RNA load, HSAECs from the same time points were lysed, viral RNA extracted and analyzed by qRT-PCR. The intracellular viral genomic copies in Bortezomib treated cells followed the same decreasing trend as we observed with the extracellular virions (Figure 2B).

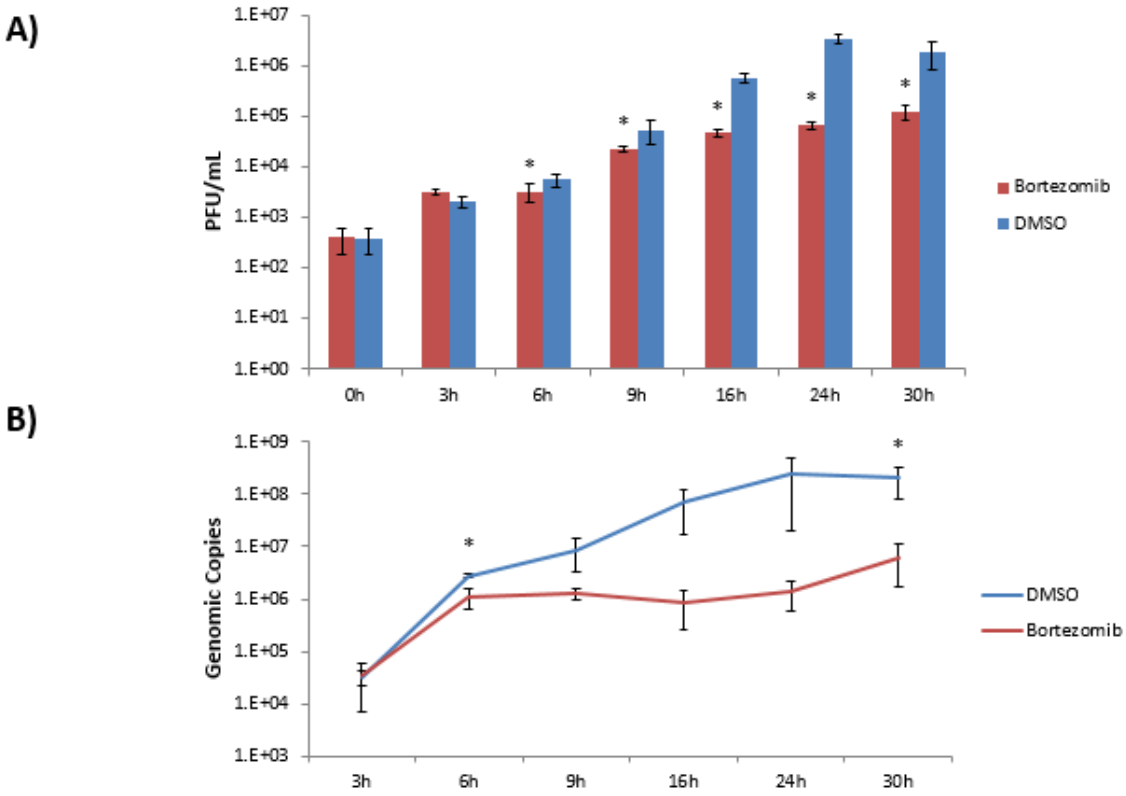

Figure 2: Bortezomib decreases viral load in an intracellular and extracellular manner. (A). HSAECs were pre-treated with DMSO or Bortezomib and cells were infected with rMP-12 (MOI 0.1) for 1 hour. Supernatants were collected at defined intervals from 0hpi to 30hpi to be analyzed via plaque assay. Results are an average of 2 independent experiments with biological triplicates. **(B).** Pretreated HSAECs were infected with rMP-12 (MOI 0.1). Supernatants were removed at defined intervals, cells were lysed and total RNA isolated. Levels of viral RNA were quantified by qRT-PCR using M-segment specific primers. Results are representative of 2 independent experiments with biological triplicates. * indicates $P<0.05$.

Next, we determined post exposure efficacy of Bortezomib in inhibiting MP-12 multiplication. HSAECs were infected with rMP-12 without pretreatment, and then treated with Bortezomib at 2, 4, 6 and 8 hpi. Supernatants were collected at 24 hours and infectious viral titers determined. Our results indicated that treatment with Bortezomib up to 6 hpi resulted in at least a 1 log decrease in extracellular viral titers (Figure 3A). Cumulatively, our data indicated that at nontoxic concentrations, Bortezomib was capable of inhibiting MP-12 multiplication in infected cells.

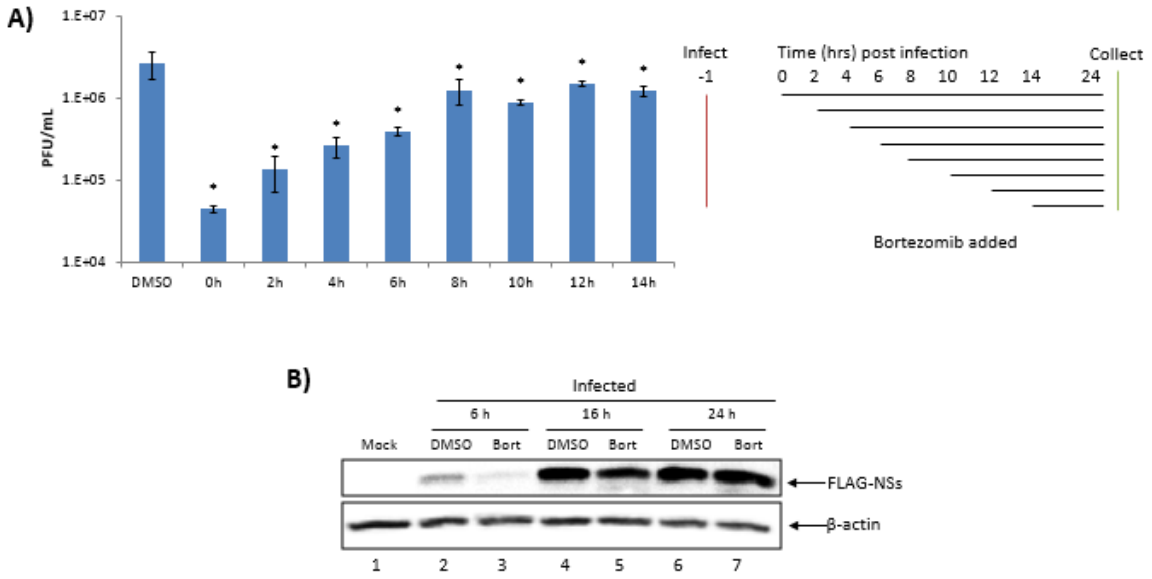

Figure 3: Bortezomib treatment most effective during early stages of viral infection. (A). HSAEC were infected with rMP-12 (MOI 0.1) for 1 hour. Viral inoculum was then removed and replaced with either 0.1% DMSO treated or untreated HSAEC media. At 2 hour intervals, media were replaced with media containing 0.01μM Bortezomib. Representative schematic of the assay is provided. Supernatants were collected at 24hpi and analyzed for infectious viral particles. Results are representative of 3 independent experiments with biological triplicates. **(B).** HSAECs were pre-treated followed by infection with Flag-NSs-rMP-12 (MOI 5). At defined intervals, cells were collected, lysed, and analyzed by western blot. Uninfected, untreated HSAECs were lysed at 6h as a negative control. Results are representative of 3 independent experiments. * indicates $P<0.05$.

The inhibitory effect of Bortezomib involved the viral virulence factor NSs

NSs is a critical virulence factor that is important for establishing a productive infection (Billecocq et al., 2004; Bird et al., 2008; Habjan et al., 2009; Ikegami et al., 2009a; Le May et al., 2008; Narayanan et al., 2012; Vialat et al., 2000). We hypothesized that the inhibitory potential of Bortezomib may, in part, involve an interference with known NSs-dependent phenomena in MP-12 infected cells. Before we ascribed any consequences to NSs-dependent phenomena, we wanted to determine if Bortezomib treatment resulted in any changes in NSs expression levels during the time course of infection. HSAECs were pre-treated with either DMSO or 0.01μM Bortezomib, infected with Flag-NSs-rMP-12, and total protein lysates obtained 6, 16, and 24hpi (Figure 3B). While a lag was noticed in NSs level at the 6 hour time point in the context of Bortezomib treatment, NSs levels became more comparable between DMSO and Bortezomib treated cells at the later time points tested (Figure 3B, compare lanes 4-7). We quantified the comparable NSs levels between DMSO and Bortezomib treated cells at the time points tested by measuring and averaging band intensities obtained from three independent biological repeats (Figure 3C).

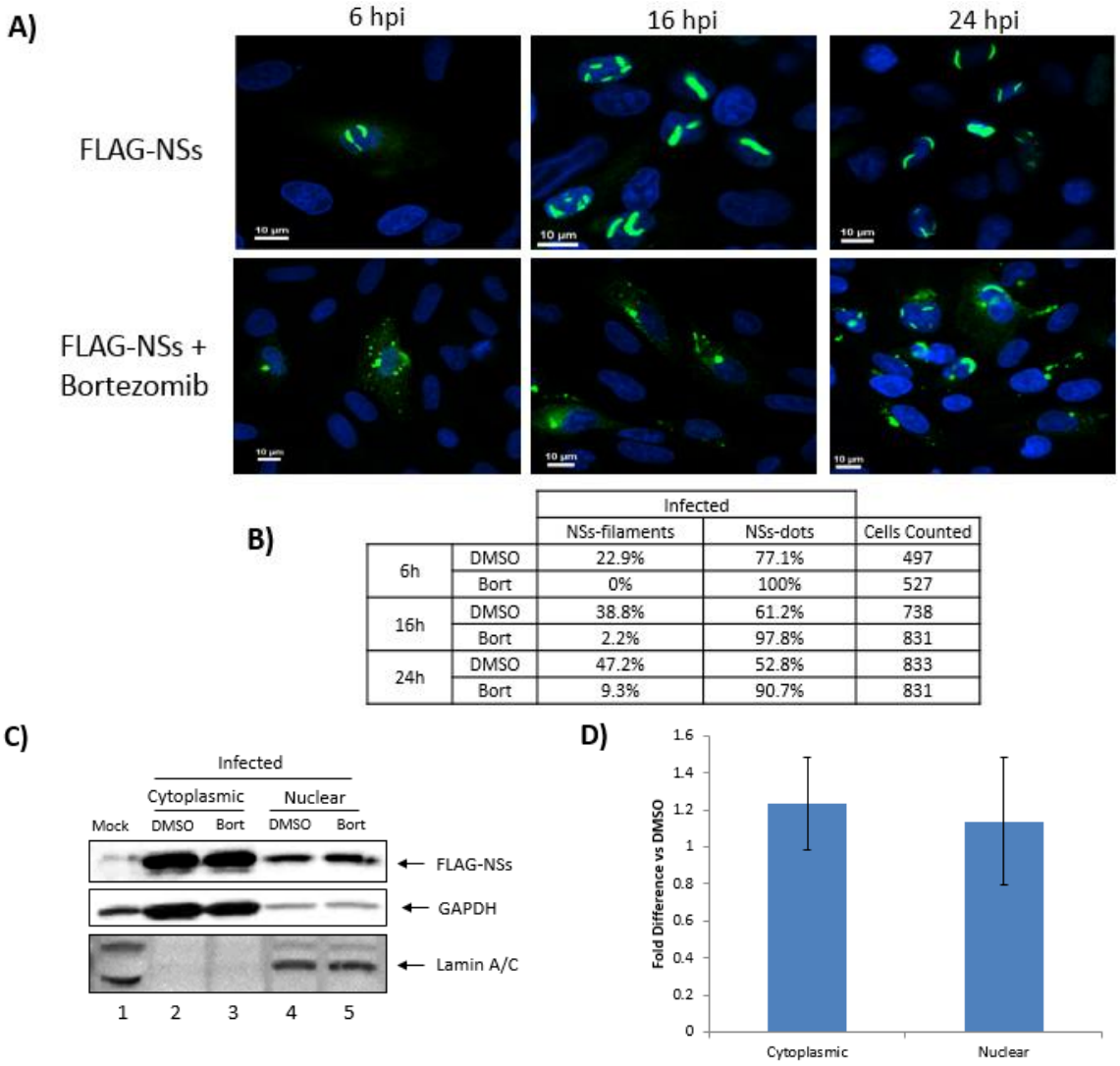

B)

		Infected		
		NSs-filaments	NSs-dots	Cells Counted
6h	DMSO	22.9%	77.1%	497
	Bort	0%	100%	527
16h	DMSO	38.8%	61.2%	738
	Bort	2.2%	97.8%	831
24h	DMSO	47.2%	52.8%	833
	Bort	9.3%	90.7%	831

Figure 4: Bortezomib robustly inhibits nuclear filament formation without affecting NSs distribution. (A). HSAECs were pre-treated with DMSO or Bortezomib. Conditioned media were removed prior to infection with Flag-NSs-rMP-12 (MOI 5). Cells were fixed and processed at 6hpi, 16hpi, and 24hpi for immunofluorescence. Results are representative of 3 independent experiments with biological triplicates. **(B).** Total counts for defined NSs phenotype (filaments or non-filamentous dots) were combined from 3 independent experiments. **(C).** HSAECs were untreated (mock) or pre-treated with DMSO or Bortezomib. The cells were infected with Flag-NSs-rMP-12 (MOI 5) or left as uninfected controls. At 16hpi, cells were collected and fractionated into cytoplasmic and nuclear fractions and analyzed by Western Blot. Images are representative of 3 independent experiments. **(D).** Signals for anti-Flag normalized to GAPDH for cytoplasmic fractions, and Lamin A/C for nuclear fractions are indicated. Differences between DMSO and Bortezomib were quantitated with Quantity One software. Results are an average of 3 independent experiments. Standard deviations were calculated accordingly

We determined if the ability of NSs to form nuclear filaments was altered in any manner in Bortezomib treated cells. We conducted immunofluorescence experiments using HSAECs infected with the Flag-NSs-rMP-12 virus, fixed at 6, 16 and 24 hpi following by probing with an anti-Flag antibody (Figure 4A). We were not able to observe NSs filaments in the Bortezomib treated cells at 6 hpi which may be partially due to the decreased amount of NSs in the treated cells at that time point. Interestingly, filament formation was compromised in Bortezomib treated cells at the 16 and 24 hpi time points as well, even though NSs levels were comparable between Bortezomib and DMSO treated cells (Figure 4A). Approximately 38% of cells showed the presence of filaments in the DMSO control while only ~2% of the Bortezomib treated cells displayed filaments at the 16 hour time point; similarly, the 24 hour time point, ~47% of the DMSO treated cells displayed filaments in the nucleus while ~9% of the Bortezomib treated cells had nuclear NSs filaments (Figure 4B). We questioned whether the inability to detect NSs filaments in the nucleus may be a reflection of a defect in nuclear transport of NSs. To that end, we fractionated cell lysates obtained from DMSO treated and Bortezomib treated cells, infected with Flag-NSs-rMP-12 virus into nuclear (N) and cytoplasmic (C) fractions. The N and C fractions were analyzed for NSs distribution. The data indicated that the total nuclear pool of NSs in Bortezomib and DMSO treated cells were comparable at the 16 hour time point (Figure 4C). We quantified the relative nuclear and cytoplasmic levels of NSs, normalizing nuclear signals to lamin and cytoplasmic signals to GAPDH, and verified that Bortezomib treatment did not exert any significant effect on the nuclear pool of NSs at the 16 hour time point. (Figures 4 C-D). Cumulatively, our

data indicated that at later time points (16 and 24 hpi), the ability of NSs to form nuclear filaments was compromised in Bortezomib treated cells.

Bortezomib treatment affects the interaction between NSs and the mSin3A-SAP30-YY1 complex.

NSs forms filamentous structures on DNA through its interactions with host repressor proteins, namely mSin3A, SAP30 and YY1 (Mansuroglu et al., 2010). We hypothesized that the lack of nuclear filaments in Bortezomib treated cells at the 16 and 24 hour time points may be the result of disruption of the interactions between NSs and the mSin3A-SAP30-YY1 complex. Previously published data had demonstrated that in the context of curcumin treatment, NSs interacted ineffectively with mSin3A (Narayanan et al., 2012). In that manuscript, the phosphorylation status of NSs mediated by a host kinase and influenced by curcumin treatment was indicated as the mechanism behind inhibition of MP-12 in infected cells. Curcumin is known to interfere with a broad array of cellular events, one of which is the inhibition of the proteasome (Milacic et al., 2008).

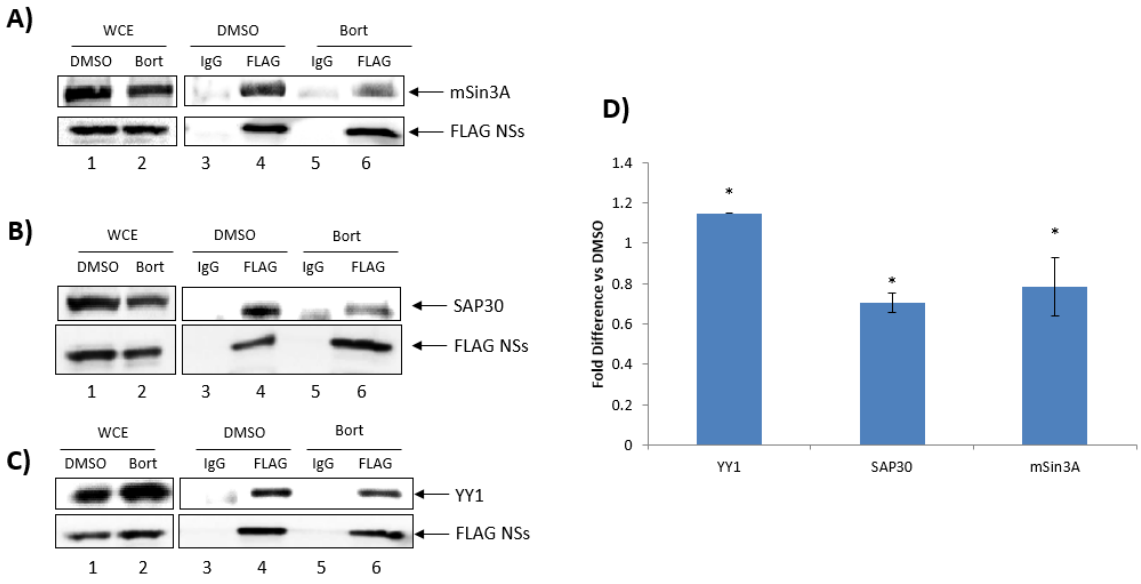

Figure 5: Bortezomib alters interaction between NSs and IFN-β repressor complex proteins. HSAECs were pre-treated with DMSO or Bortezomib prior to infection with Flag-NSs-rMP-12 (MOI 5). At 16hpi, cells were collected, lysed, and quantified. Lysates were immunoprecipitated with anti-Flag antibody and resolved by SDS-PAGE, and subsequently immunoblotted for mSin3A **(A)**, SAP30 **(B)**, and YY1 **(C)**. Blots were probed with anti-Flag as a loading control. Whole cell extract (WCE) was run separately of immunoprecipitated samples to compensate for concentration differences when imaging. Results are representative of 3 independent experiments. **(D).** Protein bands from A-C were analyzed via Quantity One software. Concentrations normalized to the total amount of NSs, and graphed as fold differences in respect to DMSO Flag readings for each experiment. Results are an average of 3 independent experiments. Standard deviations were calculated accordingly. * indicates $P<0.05$.

We investigated if Bortezomib alters the interaction between NSs and components of the mSin3A-SAP30-YY1 repressor complex. HSAECs were pre-treated with either DMSO or Bortezomib, infected with Flag-NSs-rMP-12, and total protein lysates were obtained at 16hpi for immunoprecipitation experiments. Two milligrams of total protein lysate was immunoprecipitated using anti-Flag antibodies and analyzed for co immunoprecipitation of mSin3A, YY1 and SAP30 with NSs. The experimental data indicated that Bortezomib treatment decreased the interaction of NSs with mSin3A by ~22% and SAP30 by ~ 30% (Figures 5A, B, D). The treatment, however, did not impact

the interaction of NSs with YY1 (Figure 5C). The compromised interaction of NSs with mSin3A is in agreement with the published data that curcumin treatment interfered with the NSs:mSin3A interaction (Narayanan et al., 2012). In the case of the curcumin treatment, the effect is likely mediated by both phosphorylation modifications on NSs and ubiquitination of host proteins and hence be a combinatorial effect leading to a more robust loss in interaction than what we have observed here. Bortezomib is a targeted inhibitor of the proteasome and that may explain why the effect is not as pronounced as noticed with curcumin.

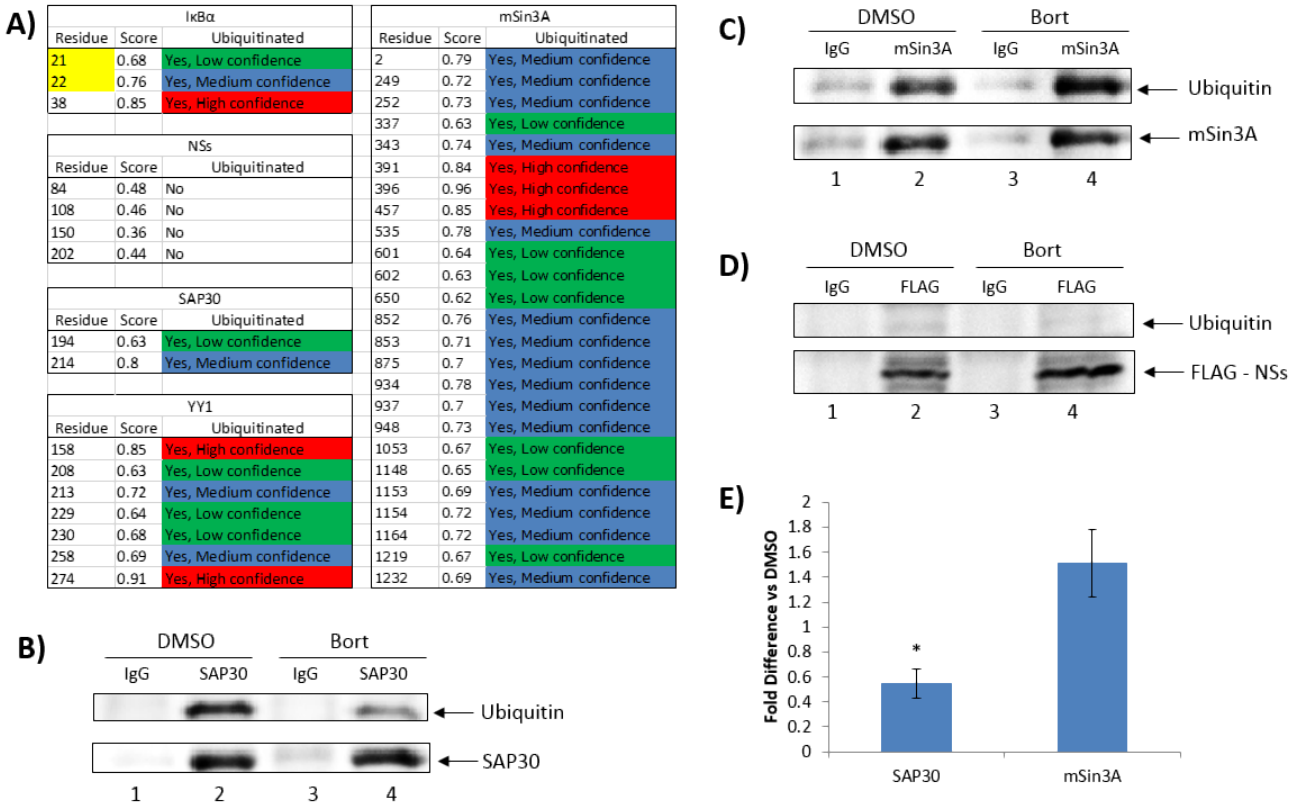

Figure 6: Bortezomib affects ubiquitination status of NSs interactors. (A). Protein sequences of known NSs interactors were analyzed via *in silico* ubiquitination prediction software Ubpred. IκBα was used as a positive control. Predicted ubiquitination sites are indicated as low, medium, and high confidence residues. **(B-D).** HSAECs were pre-treated with DMSO or Bortezomib prior to infection with Flag-NSs-rMP-12 (MOI 5). At 16hpi, cells were collected, lysed, and quantified. Lysates were immunoprecipitated with either anti-SAP30 antibody **(B)**, anti-mSin3A antibody **(C)**, or anti-Flag antibody **(D)**, resolved by SDS-PAGE, and subsequently immunoblotted for ubiquitin. Results for **B - D** are representative of 3 independent experiments. **(E).** Protein bands from **B-D** were analyzed via Quantity One software. Quantifications are represented as fold differences in respect to DMSO. * indicates $P<0.05$.

Our efforts to characterize the NSs:mSin3A-SAP30-YY1 interactions in the presence of Bortezomib led us to speculate that the ubiquitination status of the host proteins play a role in their interaction with NSs. We performed an *in silico* analysis of mSin3A, SAP30 and YY1 to query for potential ubiquitination sites using Ubiquitination

prediction (Ubpred) software (Radivojac et al., 2010). We utilized IκBα protein sequence as a positive control, as it is known to be ubiquitinated on residues 21 and 22 (Figure 6A) (Weil et al., 1997). The protein sequences of mSin3A, YY1 and SAP30 were analyzed by the prediction program which revealed multiple possible ubiquitination sites on all three proteins (Figure 6A). This observation led us to hypothesize that Bortezomib treatment altered the ubiquitination status of mSin3A and SAP30 which may contribute to the decreased interaction with NSs. We tested this hypothesis by immunoprecipitating the host proteins from infected lysates and probing for ubiquitination using anti-ubiquitin antibodies. HSAECs were treated with DMSO or Bortezomib, infected with Flag-NSs-rMP-12 virus and total protein lysates obtained at 16hpi. Two milligrams of lysate was used in an immunoprecipitation experiment using antibodies for either SAP30, or mSin3A. We immunoprecipitated NSs independently to determine if NSs was ubiquitinated. The immunoprecipitated samples were analyzed by western blot using anti-ubiquitin antibodies. We observed a statistically significant decrease in the ubiquitination of SAP30 with Bortezomib treatment (Figures 6B, E). Interestingly, we observed an increase in the association of mSin3A and ubiquitin (Figures 6C, E). This may suggest that regular ubiquitin turn over may result in a non-ubiquitinated pool of mSin3A which associated with NSs as a part of the corepressor complex. Our experiments do not determine the type of ubiquitination on mSin3A (such as K48 or K63 ubiquitination). Switching between such ubiquitination events may drive protein:protein interactions as K63 ubiquitination of proteins is known to drive protein interactions in contrast to K48 ubiquitination that targets proteins for degradation (Pickart and Fushman,

2004; Xu et al., 2009). NSs was not ubiquitinated in the infected cells regardless of Bortezomib treatment (Figure 6D). Cumulatively, the analysis of ubiquitination status of the host proteins revealed a dynamic role of ubiquitination of mSin3A and SAP30 for efficient interaction with NSs.

Bortezomib treatment increases interferon expression in MP-12 infected cells.

In combination, our demonstration that Bortezomib treatment decreased nuclear filaments and compromised association of NSs with mSin3A and SAP30 led us to propose that the treatment will result in an increase in the expression of IFN-β. To test this possibility, we measured the kinetics of IFN-β expression in DMSO treated and Bortezomib treated cells at multiple time points by qRT-PCR. Total RNA was extracted from DMSO or Bortezomib treated HSAECs at 6, 9, 16, and 24hpi with Flag-NSs-rMP-12 virus. Fold expression was calculated using the ΔΔCt method, with β-actin as the endogenous control. The results showed that IFN-β expression was higher in the Bortezomib treated cells when compared with the DMSO treated controls (Figure 7).

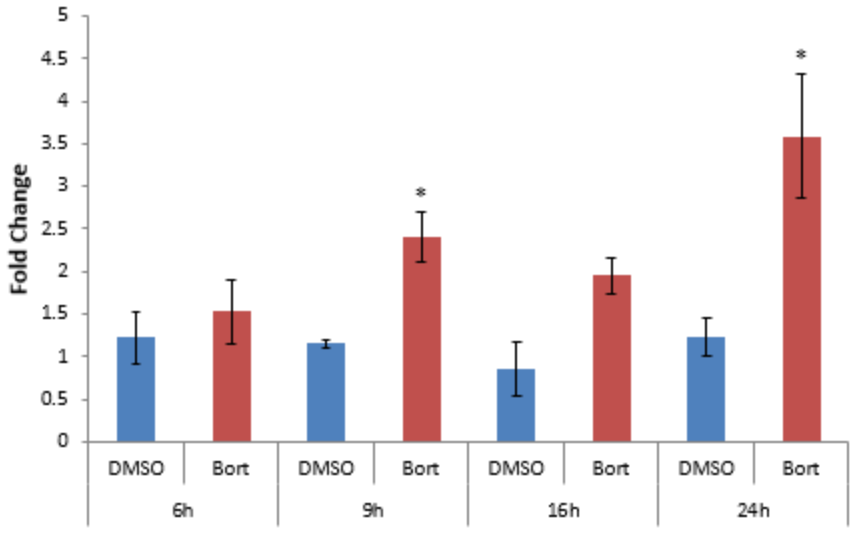

Figure 7: Bortezomib treatment allows for recovery of IFN-β expression. HSAECs were pretreated with DMSO or Bortezomib. Conditioned media was removed prior to infection with rMP-12 (MOI 0.1). Cells were lysed at defined intervals and total RNA isolated. Levels of IFN-β expression were determined by qRT-PCR and quantitated using the ΔΔCt method normalized to β-actin. Data is representative of 3 independent experiments. * indicates $P<0.05$.

Rescue of interferon expression is likely to be an outcome of multiple events that are modulated as a result of Bortezomib treatment. One such event is our observation that NSs is unable to form the repressor complex with the host proteins. It is also highly likely that incapacitating the proteasome will rescue PKR levels in the cells which will contribute to an antiviral phenotype. Finally, additional viral and host proteins will be differentially ubiquitinated during the entire infectious process, which are likely to be essential for various steps of the infectious process such as nucleocapsid degradation, RNA synthesis, viral particle assembly and egress. The consequences of Bortezomib treatment on additional viral and host proteins are part of ongoing investigations in our laboratory. In conclusion, our current studies reveal that the FDA approved proteasomal

inhibitor Bortezomib affects the ability of the viral virulence factor NSs to associate with host repressor complex components mSin3A and SAP30 by differentially modulating their ubiquitination status and hence impacting viral multiplication.

REFERENCES

Adams, J., Kauffman, M., 2004. Development of the proteasome inhibitor Velcade (Bortezomib). Cancer Invest. 22, 304–311.

Amaya, M., Voss, K., Sampey, G., Senina, S., de la Fuente, C., Mueller, C., Calvert, V., Kehn-Hall, K., Carpenter, C., Kashanchi, F., Bailey, C., Mogelsvang, S., Petricoin, E., Narayanan, A., 2014. The Role of IKKβ in Venezuelan Equine Encephalitis Virus Infection. PLoS ONE 9. doi:10.1371/journal.pone.0086745

Baer, A., Austin, D., Narayanan, A., Popova, T., Kainulainen, M., Bailey, C., Kashanchi, F., Weber, F., Kehn-Hall, K., 2012. Induction of DNA Damage Signaling upon Rift Valley Fever Virus Infection Results in Cell Cycle Arrest and Increased Viral Replication. J. Biol. Chem. 287, 7399–7410. doi:10.1074/jbc.M111.296608

Bandi, P., Garcia, M.L., Booth, C.J., Chisari, F.V., Robek, M.D., 2010. Bortezomib Inhibits Hepatitis B Virus Replication in Transgenic Mice. Antimicrob. Agents Chemother. 54, 749–756. doi:10.1128/AAC.01101-09

Billecocq, A., Spiegel, M., Vialat, P., Kohl, A., Weber, F., Bouloy, M., Haller, O., 2004. NSs Protein of Rift Valley Fever Virus Blocks Interferon Production by Inhibiting Host Gene Transcription. J. Virol. 78, 9798–9806. doi:10.1128/JVI.78.18.9798-9806.2004

Bird, B.H., Albariño, C.G., Hartman, A.L., Erickson, B.R., Ksiazek, T.G., Nichol, S.T., 2008. Rift Valley Fever Virus Lacking the NSs and NSm Genes Is Highly Attenuated, Confers Protective Immunity from Virulent Virus Challenge, and Allows for Differential Identification of Infected and Vaccinated Animals. J. Virol. 82, 2681–2691. doi:10.1128/JVI.02501-07

Bouloy, M., Weber, F., 2010. Molecular Biology of Rift Valley Fever Virus. Open Virol. J. 4, 8–14. doi:10.2174/1874357901004020008

Caplen, H., Peters, C.J., Bishop, D.H.L., 1985. Mutagen-directed Attenuation of Rift Valley Fever Virus as a Method for Vaccine Development. J. Gen. Virol. 66, 2271–2277. doi:10.1099/0022-1317-66-10-2271

Dudek, S.E., Luig, C., Pauli, E.-K., Schubert, U., Ludwig, S., 2010. The Clinically Approved Proteasome Inhibitor PS-341 Efficiently Blocks Influenza A Virus and Vesicular Stomatitis Virus Propagation by Establishing an Antiviral State. J. Virol. 84, 9439–9451. doi:10.1128/JVI.00533-10

Habjan, M., Pichlmair, A., Elliott, R.M., Overby, A.K., Glatter, T., Gstaiger, M., Superti-Furga, G., Unger, H., Weber, F., 2009. NSs Protein of Rift Valley Fever Virus Induces the Specific Degradation of the Double-Stranded RNA-Dependent Protein Kinase. J. Virol. 83, 4365–4375. doi:10.1128/JVI.02148-08

Ikegami, T., Makino, S., 2011. The Pathogenesis of Rift Valley Fever. Viruses 3, 493–519. doi:10.3390/v3050493

Ikegami, T., Narayanan, K., Won, S., Kamitani, W., Peters, C.J., Makino, S., 2009a. Dual Functions of Rift Valley Fever Virus NSs Protein: Inhibition of Host mRNA Transcription and Post-transcriptional Downregulation of Protein Kinase PKR. Ann. N. Y. Acad. Sci. 1171, E75–E85. doi:10.1111/j.1749-6632.2009.05054.x

Ikegami, T., Narayanan, K., Won, S., Kamitani, W., Peters, C.J., Makino, S., 2009b. Rift Valley Fever Virus NSs Protein Promotes Post-Transcriptional Downregulation of Protein Kinase PKR and Inhibits eIF2? Phosphorylation. PLoS Pathog. 5. doi:10.1371/journal.ppat.1000287

Indran, S.V., Ikegami, T., 2012. Novel approaches to develop Rift Valley fever vaccines. Front. Cell. Infect. Microbiol. 2. doi:10.3389/fcimb.2012.00131

Kainulainen, M., Habjan, M., Hubel, P., Busch, L., Lau, S., Colinge, J., Superti-Furga, G., Pichlmair, A., Weber, F., 2014. Virulence Factor NSs of Rift Valley Fever Virus Recruits the F-Box Protein FBXO3 To Degrade Subunit p62 of General Transcription Factor TFIIH. J. Virol. 88, 3464–3473. doi:10.1128/JVI.02914-13

Kalveram, B., Lihoradova, O., Ikegami, T., 2011. NSs Protein of Rift Valley Fever Virus Promotes Posttranslational Downregulation of the TFIIH Subunit p62. J. Virol. 85, 6234–6243. doi:10.1128/JVI.02255-10

Le May, N., Dubaele, S., De Santis, L.P., Billecocq, A., Bouloy, M., Egly, J.-M., 2004. TFIIH transcription factor, a target for the Rift Valley hemorrhagic fever virus. Cell 116, 541–550.

Le May, N., Mansuroglu, Z., Léger, P., Josse, T., Blot, G., Billecocq, A., Flick, R., Jacob, Y., Bonnefoy, E., Bouloy, M., 2008. A SAP30 Complex Inhibits IFN-β Expression in Rift Valley Fever Virus Infected Cells. PLoS Pathog. 4, e13. doi:10.1371/journal.ppat.0040013

Mansuroglu, Z., Josse, T., Gilleron, J., Billecocq, A., Leger, P., Bouloy, M., Bonnefoy, E., 2010. Nonstructural NSs Protein of Rift Valley Fever Virus Interacts with Pericentromeric DNA Sequences of the Host Cell, Inducing Chromosome Cohesion and Segregation Defects. J. Virol. 84, 928–939. doi:10.1128/JVI.01165-09

Milacic, V., Banerjee, S., Landis-Piwowar, K.R., Sarkar, F.H., Majumdar, A.P.N., Dou, Q.P., 2008. Curcumin inhibits the proteasome activity in human colon cancer cells in vitro and in vivo. Cancer Res. 68, 7283–7292. doi:10.1158/0008-5472.CAN-07-6246

Narayanan, A., Amaya, M., Voss, K., Chung, M., Benedict, A., Sampey, G., Kehn-Hall, K., Luchini, A., Liotta, L., Bailey, C., Kumar, A., Bavari, S., Hakami, R.M., Kashanchi, F., 2014. Reactive oxygen species activate NFκB (p65) and p53 and induce apoptosis in RVFV infected liver cells. Virology 449, 270–286. doi:10.1016/j.virol.2013.11.023

Narayanan, A., Kehn-Hall, K., Senina, S., Lundberg, L., Van Duyne, R., Guendel, I., Das, R., Baer, A., Bethel, L., Turell, M., Hartman, A.L., Das, B., Bailey, C., Kashanchi, F., 2012. Curcumin Inhibits Rift Valley Fever Virus Replication in Human Cells. J. Biol. Chem. 287, 33198–33214. doi:10.1074/jbc.M112.356535

Narayanan, A., Popova, T., Turell, M., Kidd, J., Chertow, J., Popov, S.G., Bailey, C., Kashanchi, F., Kehn-Hall, K., 2011. Alteration in superoxide dismutase 1 causes oxidative stress and p38 MAPK activation following RVFV infection. PloS One 6, e20354. doi:10.1371/journal.pone.0020354

Nuss, J.E., Kehn-Hall, K., Benedict, A., Costantino, J., Ward, M., Peyser, B.D., Retterer, C.J., Tressler, L.E., Wanner, L.M., McGovern, H.F., Zaidi, A., Anthony, S.M., Kota, K.P., Bavari, S., Hakami, R.M., 2014. Multi-Faceted Proteomic Characterization of Host Protein Complement of Rift Valley Fever Virus Virions and Identification of Specific Heat Shock Proteins, Including HSP90, as Important Viral Host Factors. PLoS ONE 9. doi:10.1371/journal.pone.0093483

Pepin, M., Bouloy, M., Bird, B.H., Kemp, A., Paweska, J., 2010. Rift Valley fever virus (Bunyaviridae: Phlebovirus): an update on pathogenesis, molecular epidemiology, vectors, diagnostics and prevention. Vet. Res. 41. doi:10.1051/vetres/2010033

Pickart, C.M., Fushman, D., 2004. Polyubiquitin chains: Polymeric protein signals. Curr. Opin. Chem. Biol. 8, 610–616. doi:10.1016/j.cbpa.2004.09.009

Popova, T.G., Turell, M.J., Espina, V., Kehn-Hall, K., Kidd, J., Narayanan, A., Liotta, L., Petricoin, E.F., Kashanchi, F., Bailey, C., Popov, S.G., 2010. Reverse-Phase Phosphoproteome Analysis of Signaling Pathways Induced by Rift Valley Fever

Virus in Human Small Airway Epithelial Cells. PLoS ONE 5. doi:10.1371/journal.pone.0013805

Raaben, M., Posthuma, C.C., Verheije, M.H., te Lintelo, E.G., Kikkert, M., Drijfhout, J.W., Snijder, E.J., Rottier, P.J.M., de Haan, C.A.M., 2010. The Ubiquitin-Proteasome System Plays an Important Role during Various Stages of the Coronavirus Infection Cycle. J. Virol. 84, 7869–7879. doi:10.1128/JVI.00485-10

Radivojac, P., Vacic, V., Haynes, C., Cocklin, R.R., Mohan, A., Heyen, J.W., Goebl, M.G., Iakoucheva, L.M., 2010. Identification, analysis, and prediction of protein ubiquitination sites. Proteins 78, 365–380. doi:10.1002/prot.22555

Shafagati, N., Narayanan, A., Baer, A., Fite, K., Pinkham, C., Bailey, C., Kashanchi, F., Lepene, B., Kehn-Hall, K., 2013. The Use of NanoTrap Particles as a Sample Enrichment Method to Enhance the Detection of Rift Valley Fever Virus. PLoS Negl. Trop. Dis. 7. doi:10.1371/journal.pntd.0002296

Struthers, J.K., Swanepoel, R., 1982. Identification of a Major Non-structural Protein in the Nuclei of Rift Valley Fever Virus-infected Cells. J. Gen. Virol. 60, 381–384. doi:10.1099/0022-1317-60-2-381

Swanepoel, R., Blackburn, N.K., 1977. Demonstration of Nuclear Immunofluorescence in Rift Valley Fever Infected Cells. J. Gen. Virol. 34, 557–561. doi:10.1099/0022-1317-34-3-557

Teale, A., Campbell, S., Van Buuren, N., Magee, W.C., Watmough, K., Couturier, B., Shipclark, R., Barry, M., 2009. Orthopoxviruses Require a Functional Ubiquitin-Proteasome System for Productive Replication. J. Virol. 83, 2099–2108. doi:10.1128/JVI.01753-08

Vialat, P., Billecocq, A., Kohl, A., Bouloy, M., 2000. The S Segment of Rift Valley Fever Phlebovirus (Bunyaviridae) Carries Determinants for Attenuation and Virulence in Mice. J. Virol. 74, 1538–1543.

Vialat, P., Muller, R., Vu, T.H., Prehaud, C., Bouloy, M., 1997. Mapping of the mutations present in the genome of the Rift Valley fever virus attenuated MP12 strain and their putative role in attenuation. Virus Res. 52, 43–50. doi:10.1016/S0168-1702(97)00097-X

Wang, Y.E., Park, A., Lake, M., Pentecost, M., Torres, B., Yun, T.E., Wolf, M.C., Holbrook, M.R., Freiberg, A.N., Lee, B., 2010. Ubiquitin-Regulated Nuclear-Cytoplasmic Trafficking of the Nipah Virus Matrix Protein Is Important for Viral Budding. PLoS Pathog. 6. doi:10.1371/journal.ppat.1001186

Weil, R., Laurent-Winter, C., Israël, A., 1997. Regulation of IκBβ Degradation SIMILARITIES TO AND DIFFERENCES FROM IκBα. J. Biol. Chem. 272, 9942–9949. doi:10.1074/jbc.272.15.9942

Xu, P., Duong, D.M., Seyfried, N.T., Cheng, D., Xie, Y., Robert, J., Rush, J., Hochstrasser, M., Finley, D., Peng, J., 2009. Quantitative Proteomics Reveals the Function of Unconventional Ubiquitin Chains in Proteasomal Degradation. Cell 137, 133–145. doi:10.1016/j.cell.2009.01.041

BIOGRAPHY

Forrest David Keck graduated from the International Baccalaureate program at Princess Anne High School, Virginia Beach, Virginia, in 2010. He received his Bachelor of Science in Biology from George Mason University in 2013. He was employed as a graduate teaching assistant at George Mason for a year while receiving his Master of Science in Biology, with a concentration in Microbiology and Infectious Diseases from George Mason University in 2015.